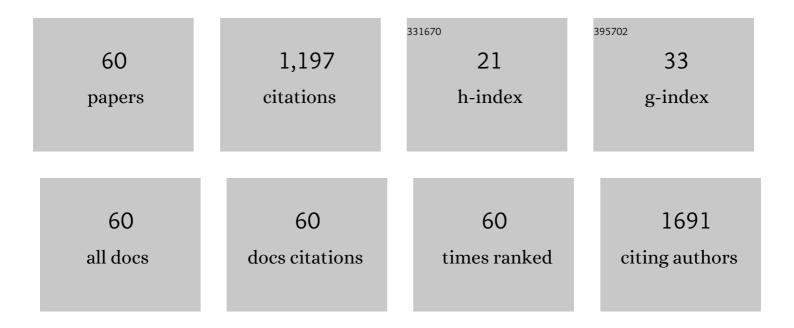
Xiangli Zhong

List of Publications by Year in descending order

Source: https://exaly.com/author-pdf/3659737/publications.pdf Version: 2024-02-01



XIANCU ZHONG

#	Article	IF	CITATIONS
1	Electrically driven motion, destruction, and chirality change of polar vortices in oxide superlattices. Science China: Physics, Mechanics and Astronomy, 2022, 65, 1.	5.1	6
2	Improved thermal stability of AlCrSiN coatings base on the template effect of TiAlN layer. Surface Engineering, 2022, 38, 37-43.	2.2	0
3	Failure Analysis of Commercial Ferroelectric Random Access Memory for Single Event Effect. IEEE Transactions on Nuclear Science, 2022, 69, 890-899.	2.0	2
4	Significantly enhanced energy storage density and efficiency in flexible Bi3.15Nd0.85Ti3O12 thin film via periodic dielectric layers. Journal of Applied Physics, 2022, 131, .	2.5	2
5	Realization of a Flexible Humidity Sensor Based on αâ€In ₂ Se ₃ Nanosheets. ChemNanoMat, 2022, 8, .	2.8	4
6	Super-flexibility in Freestanding Single-Crystal SrRuO ₃ Conductive Oxide Membranes. ACS Applied Electronic Materials, 2022, 4, 2987-2992.	4.3	5
7	Analysis of Ion-Induced SEFI and SEL Phenomena in 90 nm NOR Flash Memory. IEEE Transactions on Nuclear Science, 2021, 68, 2508-2515.	2.0	1
8	Hydrogen-Related Recovery Effect of AlGaN/GaN High-Electron-Mobility Transistors Irradiated by High-Fluence Protons. IEEE Transactions on Nuclear Science, 2021, 68, 118-123.	2.0	12
9	Mechanical Manipulation of Nanoâ€ī winned Ferroelectric Domain Structures for Multilevel Data Storage. Advanced Functional Materials, 2021, 31, 2011029.	14.9	9
10	Theory prediction of PC3 monolayer as a promising anode material in potassium-ion batteries. Ionics, 2021, 27, 2465-2471.	2.4	7
11	Creating polar antivortex in PbTiO3/SrTiO3 superlattice. Nature Communications, 2021, 12, 2054.	12.8	50
12	High Energy Performance Ferroelectric (Ba,Sr)(Zr,Ti)O ₃ Film Capacitors Integrated on Si at 400 ŰC. ACS Applied Materials & Interfaces, 2021, 13, 22717-22727.	8.0	29
13	Prediction and experimental verification of erosion resistance of gas switch electrode materials. AIP Advances, 2021, 11, 055206.	1.3	1
14	Effects of physical properties of N-doped carbon on carbon/N-doped carbon/sulfur composite cathodes. lonics, 2021, 27, 3271.	2.4	5
15	Highly Ordered SnO2 Nanopillar Array as Binder-Free Anodes for Long-Life and High-Rate Li-Ion Batteries. Nanomaterials, 2021, 11, 1307.	4.1	12
16	Engineering polar vortex from topologically trivial domain architecture. Nature Communications, 2021, 12, 4620.	12.8	20
17	Proton-Induced Effect on AlGaN/GaN HEMTs After Hydrogen Treatment. IEEE Transactions on Device and Materials Reliability, 2021, 21, 297-302.	2.0	5
18	Hf0.5Zr0.5Oâ,,-Based Ferroelectric Field-Effect Transistors With HfOâ,, Seed Layers for Radiation-Hard Nonvolatile Memory Applications. IEEE Transactions on Electron Devices, 2021, 68, 4368-4372.	3.0	18

XIANGLI ZHONG

#	Article	IF	CITATIONS
19	Probing Ultrafast Dynamics of Ferroelectrics by Timeâ€Resolved Pumpâ€Probe Spectroscopy. Advanced Science, 2021, 8, e2102488.	11.2	19
20	Large-scale multiferroic complex oxide epitaxy with magnetically switched polarization enabled by solution processing. National Science Review, 2020, 7, 84-91.	9.5	20
21	Highly Robust Flexible Ferroelectric Field Effect Transistors Operable at High Temperature with Lowâ€Power Consumption. Advanced Functional Materials, 2020, 30, 1906131.	14.9	32
22	Ferroelectric Field Effect Transistors: Highly Robust Flexible Ferroelectric Field Effect Transistors Operable at High Temperature with Lowâ€Power Consumption (Adv. Funct. Mater. 1/2020). Advanced Functional Materials, 2020, 30, 2070005.	14.9	1
23	In-Plane Strain-Modulated Photoresponsivity of the α-In ₂ Se ₃ -Based Flexible Transistor. ACS Applied Electronic Materials, 2020, 2, 140-146.	4.3	26
24	A neutron irradiation-induced displacement damage of indium vacancies in α-In ₂ Se ₃ nanoflakes. Physical Chemistry Chemical Physics, 2020, 22, 15799-15804.	2.8	9
25	γ-ray Radiation on Flexible Perovskite Solar Cells. ACS Applied Energy Materials, 2020, 3, 7318-7324.	5.1	27
26	Atomic-scale observations of electrical and mechanical manipulation of topological polar flux closure. Proceedings of the National Academy of Sciences of the United States of America, 2020, 117, 18954-18961.	7.1	41
27	Flexible electronic synapse enabled by ferroelectric field effect transistor for robust neuromorphic computing. Applied Physics Letters, 2020, 117, .	3.3	57
28	Superparaelectric (Ba _{0.95} ,Sr _{0.05})(Zr _{0.2} ,Ti _{0.8})O ₃ Ultracapacitors. Advanced Energy Materials, 2020, 10, 2001778.	19.5	69
29	Epitaxial array of Fe3O4 nanodots for high rate high capacity conversion type lithium ion batteries electrode with long cycling life. Nano Energy, 2020, 74, 104876.	16.0	51
30	Pore-making ionic liquid drived carbon as polar mixture for carbon/sulfur composite cathodes. Ionics, 2020, 26, 2949-2957.	2.4	0
31	Effect of interfacial delamination on coating crack in thick diamond-like carbon coatings under indentation. Acta Mechanica Sinica/Lixue Xuebao, 2020, 36, 524-535.	3.4	6
32	The total dose effect of γ-ray induced domain evolution on α-In ₂ Se ₃ nanoflakes. Physical Chemistry Chemical Physics, 2020, 22, 7160-7164.	2.8	10
33	Negative differential resistance effect in resistive switching devices based on h-LuFeO ₃ /CoFe ₂ O ₄ heterojunctions. Physical Chemistry Chemical Physics, 2020, 22, 5819-5825.	2.8	17
34	An Effective Strategy for Photoelectric Performance Enhancement of 2D Perovskite via Halogenating Organic Cation: A Theoretical Prediction. Physica Status Solidi (B): Basic Research, 2020, 257, 1900599.	1.5	1
35	Atomic imaging of mechanically induced topological transition of ferroelectric vortices. Nature Communications, 2020, 11, 1840.	12.8	49
36	Polar and Nonpolar Matrix Consisting of Twined Multiwalled Carbon Nanotube and High Nitrogenâ€Đoped Porous Carbon Derived from Ionic Liquid for Stable Li‧ Battery. Energy Technology, 2019, 7, 1900470.	3.8	2

XIANGLI ZHONG

#	Article	IF	CITATIONS
37	α-In ₂ Se ₃ Nanoflakes Modulated by Ferroelectric Polarization and Pt Nanodots for Photodetection. ACS Applied Nano Materials, 2019, 2, 4443-4450.	5.0	34
38	Hierarchical micro-mesoporous carbon prepared from waste cotton textile for lithium-sulfur batteries. Ionics, 2019, 25, 4057-4066.	2.4	14
39	Enhanced electromagnon excitations in Nd-doped BiFeO ₃ nanoparticles near morphotropic phase boundaries. Physical Chemistry Chemical Physics, 2019, 21, 21381-21388.	2.8	11
40	Resistive switching behavior in α-In ₂ Se ₃ nanoflakes modulated by ferroelectric polarization and interface defects. RSC Advances, 2019, 9, 30565-30569.	3.6	21
41	Subunit cell–level measurement of polarization in an individual polar vortex. Science Advances, 2019, 5, eaav4355.	10.3	31
42	An ultrathin flexible electronic device based on the tunneling effect: a flexible ferroelectric tunnel junction. Journal of Materials Chemistry C, 2018, 6, 5193-5198.	5.5	29
43	Self-assembling epitaxial growth of a single crystalline CoFe ₂ O ₄ nanopillar array <i>via</i> dual-target pulsed laser deposition. Journal of Materials Chemistry C, 2018, 6, 4854-4860.	5.5	4
44	Tuning Fe concentration in epitaxial gallium ferrite thin films for room temperature multiferroic properties. Acta Materialia, 2018, 145, 488-495.	7.9	26
45	Surface-step-terrace tuned second-order nonlinear optical coefficients of epitaxial ferroelectric BaTiO ₃ films. Journal of Materials Chemistry C, 2018, 6, 11679-11685.	5.5	11
46	(C ₆ H ₅ CH ₂ NH ₃) ₂ CuBr ₄ : A Lead-Free, Highly Stable Two-Dimensional Perovskite for Solar Cell Applications. ACS Applied Energy Materials, 2018, 1, 2709-2716.	5.1	73
47	Study of photovoltaic performance of Sb2S3/CdS quantum dot co-sensitized solar cells fabricated using iodine-based gel polymer electrolytes. Applied Physics A: Materials Science and Processing, 2018, 124, 1.	2.3	6
48	Characterization of domain distributions by second harmonic generation in ferroelectrics. Npj Computational Materials, 2018, 4, .	8.7	25
49	Deterministic, Reversible, and Nonvolatile Low-Voltage Writing of Magnetic Domains in Epitaxial BaTiO ₃ /Fe ₃ O ₄ Heterostructure. ACS Nano, 2018, 12, 9558-9567.	14.6	43
50	Organic–Inorganic Copper(II)-Based Material: A Low-Toxic, Highly Stable Light Absorber for Photovoltaic Application. Journal of Physical Chemistry Letters, 2017, 8, 1804-1809.	4.6	103
51	Epitaxial growth and magnetic properties of h-LuFeO3 thin films. Journal of Materials Science, 2017, 52, 13879-13885.	3.7	5
52	Investigation of multilevel data storage in silicon-based polycrystalline ferroelectric tunnel junction. Scientific Reports, 2017, 7, 4525.	3.3	10
53	Voltage pulse controlling multilevel data ferroelectric storage memory with a nonepitaxial ultrathin film. RSC Advances, 2016, 6, 80011-80016.	3.6	2
54	Investigation of multilevel data memory using filament and polarization control. RSC Advances, 2016, 6, 81789-81793.	3.6	2

XIANGLI ZHONG

#	Article	IF	CITATIONS
55	A ferroelectric memristor based on the migration of oxygen vacancies. RSC Advances, 2016, 6, 54113-54118.	3.6	41
56	Enhanced room temperature electrocaloric effect in barium titanate thin films with diffuse phase transition. RSC Advances, 2014, 4, 21826.	3.6	21
57	A ferroelectric tunnel junction based on the piezoelectric effect for non-volatile nanoferroelectric devices. Journal of Materials Chemistry C, 2013, 1, 418-421.	5.5	21
58	Shape-controlled hydrothermal synthesis of ferroelectric Bi4Ti3O12 nanostructures. CrystEngComm, 2013, 15, 1397.	2.6	27
59	Size effect on the ultrathin ferroelectric film directly grown on silicon for electronic devices. RSC Advances, 2013, 3, 24362.	3.6	4
60	Role of oxygen vacancies in the origin of ferromagnetism in Mnâ€doped ZnO. Crystal Research and Technology, 2011, 46, 1250-1256.	1.3	8